Gallocin A, an atypical two-peptide bacteriocin secreted by *Streptococcus gallolyticus* subsp. *gallolyticus*

Alexis Proutière, [1¶*] Laurence du Merle, [1] Marta Garcia-Lopez, [1] Corentin Léger, [2] Alexis Voegele, [2] Alexandre Chenal, [2] Antony Harrington, [3] Yftah Tal-Gan, [3,] Thomas Cokelaer, [4,5] Patrick Trieu-Cuot, [1] and Shaynoor Dramsi [1]*

[1] Institut Pasteur, Université Paris Cité, CNRS UMR6047, Biology of Gram-positive Pathogens Unit, Paris 75015 France.

[2] Institut Pasteur, Université Paris Cité, CNRS UMR3528, Biochemistry of Macromolecular Interactions Unit, Paris 75015 France

[3] University of Nevada, Reno, Department of Chemistry, Reno NV 89557, USA

[4] Institut Pasteur, Université Paris Cité, Plate-forme Technologique Biomics, F-75015 Paris, France

[5] Institut Pasteur, Université Paris Cité, Bioinformatics and Biostatistics Hub, F-75015 Paris, France

[¶] Present address: Laboratory of Molecular Microbiology, Global Health Institute, School of Life Sciences, Ecole Polytechnique Fédérale de Lausanne (EPFL), Lausanne, Switzerland.

* Correspondence: Shaynoor Dramsi, shaynoor.dramsi@pasteur.fr or Alexis Proutière alexis.proutiere@epfl.ch

Running title: Gallocin A, an atypical class IIb bacteriocin

Keywords: class IIb bacteriocin, antimicrobial peptides, immunity peptide, disulfide bond

ABSTRACT

Streptococcus gallolyticus subsp. *gallolyticus* (*SGG*) is an opportunistic gut pathogen associated with colorectal cancer. We previously showed that colonization of the murine colon by *SGG* in tumoral conditions was strongly enhanced by the production of gallocin A, a two-peptide bacteriocin. Here, we aimed at characterizing the mechanisms of its action and resistance. Using a genetic approach, we demonstrated that gallocin A is composed of two peptides, GllA1 and GllA2, which are inactive alone and act together to kill "target" bacteria. We showed that gallocin A can kill phylogenetically close relatives. Importantly, we demonstrated that gallocin A peptides can insert into membranes and permeabilize lipid bilayer vesicles. Next, we showed that the third gene of the gallocin A operon named GIP, is necessary and sufficient to confer immunity to gallocin A. Structural modelling of GllA1 and GllA2 mature peptides suggested that both peptides form alpha-helical hairpins stabilized by intramolecular disulfide bridges. The presence of a disulfide bond in GllA1 and GllA2 was confirmed experimentally. Addition of disulfide reducing agents abrogated gallocin A activity. Likewise, deletion of a gene encoding a surface protein with a thioredoxin-like domain impaired gallocin A ability to kill *Enterococcus faecalis*. Structural modelling of GIP revealed a hairpin-like structure strongly resembling that of the GllA1 and GllA2 mature peptides, suggesting a mechanism of immunity by competition with GllA1/2. Finally, identification of other class IIb bacteriocins exhibiting a similar alpha-helical hairpin fold stabilized with an intramolecular disulfide bridge suggests the existence of a new subclass of class IIb bacteriocins.

IMPORTANCE

Streptococcus gallolyticus subsp. gallolyticus (*SGG*), previously named *Streptococcus bovis* biotype I, is an opportunistic pathogen responsible for invasive infections (septicemia, endocarditis) in elderly people and often associated with asymptomatic colon tumors. *SGG* is one of the first bacteria to be associated with the occurrence of colorectal cancer in humans. Previously, we showed that tumor-associated conditions in the colon provide to *SGG* with the ideal environment to proliferate at the expense of phylogenetically and metabolically closely related commensal bacteria such as enterococci (Aymeric et al., 2017). *SGG* takes advantage of CRC-associated conditions to outcompete and substitute

32 commensal members of the gut microbiota using a specific bacteriocin named gallocin and
33 renamed gallocin A recently following the discovery of gallocin D in a peculiar *SGG* isolate.
34 Here, we showed that gallocin A is a two-peptide bacteriocin and that both GllA1 and GllA2
35 peptides are required for antimicrobial activity. Gallocin A was shown to permeabilize
36 bacterial membranes and to kill phylogenetically closely related bacteria such as most
37 streptococci, lactococci and enterococci, probably through membrane pore formation. GllA1
38 and GllA2 secreted peptides are unusually long (42 and 60 amino acids long) and with very
39 few charged amino acids compared to well-known class IIb bacteriocins. *In silico* modelling
40 revealed that both GllA1 and GllA2 exhibit a similar hairpin-like conformation stabilized by
41 an intramolecular disulfide bond. We also showed that the GIP immunity peptide also forms
42 a hairpin like structure like GllA1/GllA2. Thus, we hypothesize that GIP blocks the formation
43 of the GllA1/GllA2 complex by interacting with GllA1 or GllA2. Gallocin A may constitute the
44 first class IIb bacteriocin displaying disulfide bridges important for its structure and activity
45 and the founding member of a subtype of class IIb bacteriocins.

INTRODUCTION

Streptococcus gallolyticus subsp. *gallolyticus (SGG)*, formerly known as *S. bovis* biotype I, is a gut commensal of the rumen of herbivores causing infective endocarditis in elderly people and strongly associated with colorectal cancer (CRC). In a previous study, we have shown that *SGG* is able to take advantage of tumoral conditions (increased secondary bile salts concentration) to thrive and colonize the intestinal tract of Notch/APC mice. This colonization advantage was shown to be linked to the production of a two-component bacteriocin named gallocin enabling *SGG* to outcompete murine gut resident enterococci in tumor-bearing mice, but not in non-tumor mice (1). As such, gallocin constitutes the first bacterial factor explaining *SGG* association with CRC. Identification of a different gallocin, named gallocin D, from the environmental isolate *SGG* LL009 (2) led to renaming gallocin of *SGG* UCN34 as gallocin A.

Bacteriocins are highly diverse antimicrobial peptides secreted by nearly all bacteria. In gram-positive bacteria, they are divided in three classes based on size, amino acid composition and structure (3). Class I includes small (< 10-kDa), heat-stable peptides that undergo enzymatic modification during biosynthesis; class II includes small (< 10 kDa) heat-stable peptides without post-translational modifications; class III includes larger (> 10 kDa), thermo-labile peptides and proteins. Class II bacteriocins are further subdivided into four subtypes: class IIa consists of pediocin-like bacteriocins, class IIb consists of bacteriocins with two peptides, class IIc consists of leaderless bacteriocins, and class IId encompass all other non-pediocin-like, single peptide bacteriocins with a leader sequence. Previous *in silico* analysis revealed that gallocin A, encoded by *gallo_2021* (renamed *gllA2*) and *gallo_2020* (renamed *gllA1*), belong to the class IIb bacteriocins (Pfam10439) exhibiting a characteristic double glycine leader peptide. The third gene of this operon (*gallo_2019* renamed *gip*) was thought to encode the immunity protein.

We previously showed that a secreted peptide, GSP, activates transcription of the gallocin A core operon through a two-component system named BlpHR (4). The entire BlpHR regulon has been characterized and consists of 24 genes, of which 20 belong to the gallocin locus (4). Concomitantly, we showed that GSP but also GllA1 and GllA2 are secreted by a unique ABC transporter named BlpAB (5). GllA1 and GllA2 are synthesized as pre-peptides with an N-terminal leader sequence cleaved during export after a double glycine motif to produce

33 the extracellular mature active peptide. Well-known class IIb bacteriocins are usually
34 constituted of two genes encoding short peptides, named alpha and beta, that fold into
35 alpha-helical structures and insert into target bacterial membranes to alter their
36 permeability, resulting in ion leakage and cell death (6).

37 The aim of the present work was to characterize the gallocin A activity spectrum, its
38 mode of action and the immunity mechanism. Our results indicate that GllA1 and GllA2
39 peptides are atypical and contain a disulfide bond required for antibacterial activity. We
40 showed that GllA1/GllA2 can permeabilize lipid bilayers. The predicted structure of the GIP
41 immunity peptide strikingly mimics that of the GllA1 and GllA2 mature peptides suggesting a
42 mechanism of immunity by interference. *In vitro*, gallocin A was able to kill most closely
43 related species such as streptococci and enterococci, highlighting the potential of these
44 narrow-spectrum antimicrobials as alternatives to antibiotics.

RESULTS

Gallocin A is a two-peptide bacteriocin

As shown in Fig. 1A, the gallocin A core operon is composed of three genes (*gllA2*, *gllA1*, *gip*) coding for 2 putative bacteriocin peptides (GllA1 and GllA2) and a putative immunity protein (GIP). To demonstrate the role of *gllA1* and *gllA2* in gallocin A activity, we performed in-frame deletions of *gllA1* and *gllA2* separately in *SGG* strain UCN34 (wild-type, WT) and tested the antibacterial activity of the corresponding mutant supernatants by plate diffusion assays, as described previously (4). As shown in Fig. 1B, the antimicrobial activity of gallocin A is completely abolished in the supernatants of Δ*gllA1* and Δ*gllA2* mutants and restored when the supernatants of *ΔgllA1* and *ΔgllA2* are combined in a 1:1 ratio. This result demonstrates that both GllA1 and GllA2 are required for gallocin A activity and confirms that gallocin A is a two-peptide Class IIb bacteriocin (3). Finally, we showed that gallocin A is active in a wide range of pH (2-12, Fig. S1A) and temperature (Fig. S1B).

Since the gene encoding the putative immunity protein named GIP cannot be deleted alone without self-intoxication of the bacteria, we used the original mutant UCN34*Δblp* (1) in which the three genes of gallocin A operon (*gllA2-gllA1-gip*) were deleted and tested its sensitivity to gallocin A. As expected, the Δ*blp* mutant became sensitive to gallocin A (Fig. 1C). Next, we complemented the *Δblp* mutant with a plasmid encoding *gip* and showed that this was sufficient to restore bacterial growth of the recombinant strain in the presence of gallocin A. These results demonstrate that GIP confers immunity to gallocin A (Fig. 1C). Moreover, constitutive expression of *gip* in heterologous bacteria sensitive to gallocin (such as *Streptococcus agalactiae* and *Lactococcus lactis*) allowed their growth in the presence of gallocin (Fig. 1D). These results clearly demonstrate that expression of *gip* alone is necessary and sufficient to confer full immunity against gallocin A.

Gallocin A is active against various streptococci and enterococci

To further characterize the gallocin A activity spectrum, we tested the sensitivity of various bacteria from our laboratory collection, including species found as commensals in the gut as well as known gram-positive human pathogens. We showed that gallocin A is active only

32 against closely related bacteria, including various streptococci, enterococci, lactococci and
33 inactive against all other gram-positive and gram-negative bacteria tested (Fig. 2, Fig. S2A).
34 Interestingly, the three different *S. agalactiae* strains tested (NEM316, BM110, and A909)
35 differed significantly in their susceptibility to gallocin A. Similarly, sensitivity to gallocin A of
36 many *Enterococcus faecalis* clinical isolates, including a few vancomycin resistant isolates,
37 was also variable (Fig. S2B). These results indicate that gallocin A sensitivity of a given
38 species can vary from one strain to another.
39
40 **Gallocin A induces target cell-membrane depolarization**
41 To test whether gallocin A peptides can alter cell membrane permeability, as shown for
42 well-studied class IIb bacteriocins, we assessed its impact on target cell membrane potential
43 using the fluorescent voltage-dependent dye DiBAC4(3) and propidium iodide (PI).
44 DiBAC4(3) can access the cytoplasm only when the membrane is depolarized, thus
45 indicating an ion imbalance, and the DNA intercalator PI can only enter bacterial cells when
46 the cytoplasmic membrane is compromised. The entry of PI and DiBAC4(3) in cells exposed
47 to supernatants from UCN34 WT, Δ*blp* (no gallocin A) and Δ*blpS* (a mutant previously shown
48 to overproduce gallocin A, (4)) was assessed by flow cytometry. As shown in Fig. 3A and B,
49 fluorescent dye penetration in *E. faecalis* OG1RF was increased in the presence of gallocin A
50 as compared to the control supernatant without gallocin A, indicating that gallocin A
51 peptides can form pores in bacterial membranes.
52 It was previously shown that pore formation by the two-peptide bacteriocins lactococcin G
53 and enterocin 1071 requires the presence of UppP, a membrane protein involved in
54 peptidoglycan synthesis that could serve as a receptor for these bacteriocins (7). To
55 investigate whether gallocin A is active in the absence of a proteinaceous receptor, we
56 tested its capacity to permeabilize lipid bilayer vesicles. To do so, we used large unilamellar
57 vesicles (LUV) in which a fluorescence marker, the 8-Aminonaphthalene-1,3,6-Trisulfonic
58 Acid (ANTS) and its quencher, p-Xylene-Bis-Pyridinium Bromide (DPX), are encapsulated. If
59 pores are formed in the membrane of the liposomes, ANTS and DPX are released in the
60 medium and ANTS recovers its fluorescence. As shown in Fig. 3C, addition of UCN34 WT
61 supernatant containing gallocin A led to LUV permeabilization while the supernatant of the
62 Δ*blp* mutant had no effect, showing that gallocin A can alter the vesicle membrane. Of note,
63 addition of small amount of Tween 20 (0.01%) was necessary to observe gallocin A activity.

64 Importantly, the Δ*blp* supernatant supplemented Tween20 at 0.01% had no effect on
65 liposomes, showing that the membrane permeabilization induced by the UCN34 WT
66 supernatant is not caused by the detergent alone (Fig. 3C).
67 We also confirmed that both GllA1 and GllA2 were required for membrane
68 permeabilization. Indeed, addition of Δ*gllA1* or Δ*gllA2* supernatant alone had no effect,
69 while addition of both supernatants led to LUV permeabilization, regardless of which
70 peptide was added first (Fig. 3D).
71
72 **Gallocin A peptides contain a disulfide bond essential for their bactericidal activity**
73 Both GllA1 and GllA2 pre-peptides exhibit a typical N-terminal leader sequences of 23 amino
74 acids, ending with two glycine residues, which is cleaved upon secretion of these peptides
75 through a dedicated ABC transporter (5). GllA1 and GllA2 mature peptides each contain 2
76 cysteines, which can potentially form a disulfide bridge important for their structure and
77 function. Indeed, we showed that addition of reducing agents such as dithiothreitol (DTT) or
78 β-mercaptoethanol (data not shown) abolished gallocin A activity (Fig. 4A), whereas it has
79 no effect on a control bacteriocin which does not possess a disulfide bond, such as nisin.
80 Furthermore, LC/MS analysis provided the exact molecular masses of the mature GllA1 and
81 GllA2 peptides. The calculated masses identified oxidized cysteine residues, indicating the
82 presence of a disulfide bridge in each peptide (Fig. S3).
83 Interestingly, the gallocin A genomic locus in *SGG* UCN34 contains a conserved co-
84 regulated gene (4), *gallo_rs10370*, encoding a putative "bacteriocin biosynthesis protein"
85 containing a thioredoxin domain (Fig. 4B). The thioredoxin domain is known to facilitate
86 disulfide bond formation in *E. coli* (8) and is predicted to be extracellular by
87 Pfam/Interproscan. We hypothesized that this gene renamed *blpT*, which encodes a surface
88 protein potentially anchored to the cell-wall, could assist disulfide bond formation in
89 gallocin A peptides following secretion and cleavage of the leader peptide by the ABC
90 transporter BlpAB (5). Indeed, deletion of this gene in UCN34 (Δ*blpT*) strongly altered the
91 ability of *SGG* to outcompete *Enterococcus faecalis* OG1RF in competition experiments
92 where attacker *SGG* and prey *E. faecalis* were inoculated together in THY liquid medium at a
93 1:1 ratio and counted on entero-agar plates after 4 h of co-culture at 37°C (Fig. 4C).
94 Remarkably, the Δ*blpT* mutant was comparable to the Δ*blp* mutant and the back to the WT
95 behaved like the parental UCN34 WT (Fig. 4C). Altogether these results indicate the

96 existence of disulfide bond in gallocin A mature peptides important for activity. Of note, the
97 disulfide bond formation pathway of *E. coli*, containing the thioredoxin-like protein DsbA,
98 was shown to be particularly important in anaerobic conditions (9). It is thus tempting to
99 speculate that BlpT activity could be particularly important in the anaerobic environment
100 that *SGG* encounter in the colon.
101
102
103 **The structural models of gallocin A peptides differ from those of other two-peptide**
104 **bacteriocins.**
105 Structural modelling of GllA1 and GllA2 pre- and mature forms was performed using
106 ColabFold (10) and showed that the putative N-terminal leader sequences adopt disordered
107 and extended conformations (Fig. 5A and B). The structural models of mature GllA1 and
108 GllA2 are composed of two antiparallel alpha-helices, i.e. adopting an alpha-helical hairpin
109 fold (Fig. 5A and B and Fig. S4A and B). Interestingly, the two cysteines of GllA1 and GllA2
110 are facing one other in each alpha-helix of the helical hairpins, forming an intramolecular
111 disulfide bond. This suggests that the disulfide bonds in GllA1 and GllA2 reduce the
112 conformational flexibility within each alpha-helical hairpin and stabilize their three-
113 dimensional structures. Interestingly, modelling of the immunity peptide GIP shows striking
114 structural similarities with those of the mature GllA1 and GllA2 peptides (Fig. 6A and Fig.
115 S4C). Despite a relative low confidence (lDDT between 50 and 65 %), the five structural
116 models of GllA1/GllA2, GllA1/GIP and GllA2/GIP show similar orientations, giving credit to
117 these models (Fig. 6B-D and Fig. S4D- F). As shown by aligning Cα of each GIP in the
118 GllA1/GIP and GllA2/GIP, we hypothesized that GIP could intercalate between GllA1 and
119 GllA2 (Fig. 6E). Thus, GIP might provide immunity by preventing interaction between GllA1
120 and GllA2 within the bacterial cell membrane of the producing bacteria.
121
122 **Mechanisms of resistance to gallocin A**
123 To better understand the mode of action of gallocin A, we decided to investigate the
124 mechanisms of resistance to gallocin A. For that purpose, we isolated 14 spontaneous
125 mutants (named RSM 1 to 14) of the highly sensitive strain *S. gallolyticus* subsp.
126 *macedonicus* CIP 105683T on agar plates supplemented with gallocin A (see Materials and
127 Methods for details). As shown in the supplemental Fig. S5B and C, 12 out of these 14

128 mutants were able to grow in liquid THY supplemented with gallocin A, in contrast to the
129 parental strain *SGM* WT. However, when grown in presence of the control *Δblp* supernatant,
130 which does not contain gallocin A, all the mutants exhibited a longer latency phase than the
131 parental *SGM* WT, suggesting that the acquired mutations may have a fitness cost.
132 To identify the mutations conferring resistance to gallocin A in these mutants, whole-
133 genome sequencing was performed using Illumina technology and compared with the
134 genome of the parental strain that was *de novo* assembled using PacBio sequencing.
135 Between 1 and 8 single nucleotide polymorphism (SNP)/deletion/insertion were identified
136 in each RSM mutant when compared to the WT controls (Table 1). Seven out of twelve
137 mutants (RSM1, RSM2, RSM4, RSM5, RSM6, RSM12, RSM14) had mutations in the genes
138 encoding the WalKR two-component system (TCS) and 3 others (RSM 7, RSM 8 and RSM10)
139 had mutations in a gene (homologous to *gallo_rs1495*) encoding a putative "aggregation
140 promoting factor" which contain a LysM peptidoglycan-binding domain and a lysozyme-like
141 domain (Table 1, Fig. S6). The 2 remaining mutants (RSM3 and RSM11) displayed mutations
142 which were not present in the other mutants and located in other genes.
143 The WalRK TCS is known as the master regulator of cell wall homeostasis, cell membrane
144 integrity, and cell division processes in gram-positive bacteria (11). In streptococci, response
145 regulator WalR (VicR) but not the histidine kinase WalK (VicK) is essential. Consistent with
146 this, the 2 mutations observed in WalR were single amino acid substitutions (RSM6 Ala_{95} to
147 Val; RSM12 Arg_{117} to Cys) while 4 out of the 5 mutations in WalK led to a frameshift or the
148 appearance of a STOP codon (Fig. S6).
149 Interestingly, three other mutants (RSM7, RSM8 and RSM10) mapped in a single gene
150 encoding a putative cell-wall binding protein with a C-terminal lysozyme-like domain. Two
151 mutants (RSM7 and RSM8) exhibited frameshift mutations leading to the appearance of a
152 premature STOP codon, and the last one (RSM10) a substitution of the putative key catalytic
153 residue of the lysozyme-like domain (E_{137} to K, Fig. S6).
154 Thus, we hypothesized that peptidoglycan alterations in these mutant strains could explain
155 the resistance to gallocin A. To test this hypothesis, we labelled peptidoglycan with the
156 fluorescent lectin Wheat Germ Agglutinin (WGA-488) and imaged the mutants with
157 conventional fluorescence microscopy. As shown in Fig. 7, most gallocin A resistant mutants,
158 including all WalKR mutants, exhibit abnormal morphology and formed small aggregates as
159 compared to the typical *SGM* WT linear chain of 2-5 cells. Cell morphology defects and

160 peptidoglycan alterations were also detected in the 2 mutants which do not share common
161 mutations with the other mutants (RSM 3 and 13, Fig. 7).
162 Taken together, these results suggest that alteration of the peptidoglycan structure could
163 lead to gallocin A resistance, either by blocking its access to the membrane or by the
164 formation of cell aggregates. It is worth noting that RSM mutants' resistance to gallocin A
165 was intermediate and that no potential membrane receptor for gallocin A peptides was
166 identified.

DISCUSSION

Gallocin A is a class IIb bacteriocin secreted by *Streptococcus gallolyticus* subsp. *gallolyticus* (*SGG*) to outcompete indigenous gut *Enterococcus faecalis* (*EF*) in tumoral conditions only (1). Mechanistically, gallocin A activity was found to be enhanced by higher concentrations of secondary bile acids found in tumoral conditions (1). Another proof-of-concept study showed that *EF* carrying the conjugative plasmid pPD1 expressing bacteriocin was able to replace indigenous enterococci lacking pPD1 (11). The rise of antimicrobial resistance combined with the recognized roles in health of gut microbiota homeostasis has attracted a renewed interest in the role of bacteriocins in gut colonization and their use as potential tools for editing and shaping the gut microbiome (12).

We show here that gallocin A, like many class IIb bacteriocins, only kills closely related species belonging to the Streptococcaceae and Enterococcaceae family. Interestingly, gallocin A can kill *Enterococcus faecium*, a commensal bacterium contributing largely to the transfer of antibiotic resistance in the microbiome and classified as high priority in the "WHO priority pathogens list for R&D of new antibiotics". Taken together, these results highlight the potential of using bacteriocins such as gallocin A to fight antibiotic resistance and to cure bacterial infections with a lower impact on the gut microbiota due to their narrow spectrum of action.

Both GllA1 and GllA2 are synthesized as pre-peptides with an N-terminal leader sequence which is cleaved during export after a GG motif via a specific ABC transporter, BlpAB, to produce the extracellular mature active peptides (5). Experimental determination of the molecular mass of GllA1 and GllA2 by LC/MS fits with a cleavage after the GG motif present in the leader sequence and indicates the presence of an intramolecular disulfide bond in GllA1 and GllA2. Moreover, reduction of these disulfide bonds abrogates gallocin A antimicrobial activity. ColabFold modeling of GllA1 and GllA2 indicates that the N-terminal leader sequence is unstructured and that the mature GllA1 and GllA2 share a similar structural fold with two antiparallel α-helices forming a hairpin stabilized by an intramolecular disulfide bond. To our knowledge, this is the first report of an intramolecular disulfide bond in class IIb bacteriocin peptides. Most class IIb peptides, including the well

33 described lactococcin G, the plantaricin EF, the plantaricin JK and the carnobacteriocin XY
34 (CbnXY) (13–16)**,** do not contain cysteine residues in their primary amino acid sequences.
35 Consistently, the peptides constituting these 4 well-known bacteriocins are composed of
36 only one main alpha-helix, and therefore do not require any disulfide bond to stabilize their
37 tri-dimensional structures. Recently, gallocin D was identified in a very peculiar strain *SGG*
38 LL009, isolated from raw goat milk in New Zealand (2). Gallocin D is a two-peptide
39 bacteriocin homologous to infantaricin A secreted by *Streptococcus infantarius*, a member
40 of the *Streptococcus bovi*s group (2). Of note, the peptides of the 4 well described two-
41 peptide bacteriocins discussed above and of gallocin D are much smaller in size (about 30
42 amino acids long) than the gallocin A peptides (2). In addition, gallocin A peptides are less
43 positively charged (1 positively charged amino acid in GllA1, 2 in GllA2), while the highly
44 positively charged C-terminus of lactococcin G α-peptide is thought to contribute to the
45 anchoring of the peptide to the membrane, thanks to the transmembrane potential
46 (negative inside) (13, 17).
47 A few other class IIb bacteriocins, such as brochocin C, thermophilin 13 and ABP-118
48 (18–21)**,** were found to share similar structural properties with gallocin A peptides (longer
49 peptides, few positively charged amino acids and two cysteine residues in each peptide
50 located close to N-/C-terminus). Alphafold modelling of these peptides showed that their
51 putative structures resemble those of GllA1 and GllA2, with two-antiparallel alpha-helices.
52 Disulfide bonds between the cysteines of the 2 helices were also predicted in 5 out of the 6
53 peptides (Fig. S7). BrcB, the peptide without predicted disulfide bond, was also the one with
54 the worse IDDT score, suggesting that the prediction might not be accurate. In conclusion,
55 gallocin A, as well as other class IIb bacteriocins such as brochocin C, thermophilin 13 and
56 ABP-118, might represent a subgroup in class IIb bacteriocins which differs in structure, and
57 potentially in their mode of action from the other well-known class IIb bacteriocins.
58
59 Finally, gallocin A resistance was studied through whole-genome sequencing of 12
60 spontaneous resistant mutants derived from the highly sensitive strain *S. gallolyticus* subsp.
61 *macedonicus* CIP105683T. Previously, this method allowed the identification of UppP as a
62 membrane receptor required for lactococcin G activity (7). Unlike this previous study, we did
63 not find a common gene mutated in our 12 resistant mutants (RSM), suggesting that gallocin
64 A does not require the presence of a specific receptor. This is in agreement with our data

65 showing that gallocin A can permeabilize lipid vesicles composed of two phospholipids
66 (phosphatidylcholine and phosphatidylglycerol). The majority of RSM mutants exhibited
67 mutations in the genes encoding a regulatory two-component system sharing strong
68 homologies with WalKR (also known as VicKR and YycGF). This two-component system,
69 originally identified in *Bacillus subtilis*, is very highly conserved and specific to low GC%
70 Gram-positive bacteria, including several pathogens such as *Staphylococcus aureus* **(22, 23).**
71 Several studies have unveiled a conserved function for this system in different bacteria,
72 including several streptococcal pathogens, defining this signal transduction pathway as a
73 master regulatory system for cell wall metabolism **(23)**. Consistent with the potential defect
74 in cell-wall synthesis, these mutants showed morphological abnormalities and cell-division
75 defects. Similar observations have been reported in *Staphylococcus aureus* (24–26) where
76 mutations in *walK* were shown to confer intermediate resistance to vancomycin and
77 daptomycin.

78 Three mutants displayed independent mutations in a small protein (197 amino acids)
79 of unknown function containing an N-terminus LysM-peptidoglycan binding domain and a C-
80 terminus lysozyme-like domain. The lysozyme-like domain, which is about fifty amino acids
81 long, was originally identified in enzymes that degrade the bacterial cell-walls. Interestingly,
82 the mutations in RSM7, RSM8, RSM10 mutant all mapped within the lysozyme-like domain,
83 suggesting a potential alteration of the cell-wall in these mutants. Finally, the last two last
84 mutants (RSM3 and RSM13) carrying mutations in other genes than in *walRK* exhibited the
85 same morphology defects associated with gallocin A resistance.

86 To conclude, it is worth highlighting that the 12 mutants were only partially resistant
87 to gallocin A. Most RSM mutants form bacterial aggregates which probably contributes to
88 their resistance to gallocin A, just as biofilms are more resistant to antibiotics. No specific
89 membrane receptor could be identified for gallocin A. Interestingly, it has also been
90 suggested that thermophilin 13, another class IIb bacteriocin that shares putative structural
91 similarity with gallocin A (18), does not require any specific receptor for its activity.
92 However, the different level of susceptibility to gallocin A within a given species, as
93 demonstrated for three Group B *Streptococcus* strains (A909 > BM110> NEM316), as well as
94 its narrow-spectrum mode of action indicate that unidentified bacterial factors can
95 modulate gallocin A sensitivity. It will also be important in the future to identify the direct

96 bacterial targets of gallocin A in the murine colon using global 16S DNA sequencing in
97 normal and tumoral conditions.

MATERIALS AND METHODS

Cultures, bacterial strains, plasmids and oligonucleotides

Streptococci and *Enterococci* used in this study were grown at 37°C in Todd-Hewitt broth supplemented with 0.5% yeast extract (THY) in standing filled flasks. When appropriate, 10 µg/mL of erythromycin were added for plasmid maintenance.

Plasmid construction was performed by: PCR amplification of the fragment to insert in the plasmid with Q5® High-Fidelity DNA Polymerase (New England Biolabs), digestion with the appropriate FastDigest restriction enzymes (ThermoFisher), ligation with T4 DNA ligase (New England Biolabs) and transformation in commercially available TOP10 competent *E. coli* (ThermoFisher). *E. coli* transformants were cultured in Miller's LB supplemented with 150 µg/mL erythromycin (for pG1- derived plasmids) or 50 µg/mL kanamycin (pTCV- derived plasmid). Verified plasmids were electroporated in *S. agalactiae* NEM316 and mobilized from NEM316 to *SGG* UCN34 by conjugation as described previously (27). pTCV-derived plasmids were electroporated in *Lactococcus lactis* NZ9000. Strains, plasmids and primers used in this study are listed in Table 1. The wide range of bacteria tested *in vitro* for their resistance or sensitivity to gallocin A antimicrobial activity come from our laboratory repository and were cultured in their optimal media and conditions.

Construction of markerless deletion mutants in *SGG* UCN34

In-frame deletion mutants were constructed as described previously (27). Briefly, the 5' and 3' region flanking the region to delete were amplified and assembled by splicing by overlap extension PCR and cloned into the thermosensitive shuttle vector pG1. Once transformed in UCN34, the cells were cultured at 38°C with erythromycin to select for the chromosomal integration of the plasmid by homologous recombination. About 4 single cross-over integrants were serially passaged at 30 °C without antibiotic to facilitate the second event of homologous recombination and excision of the plasmid resulting either in gene deletion or back to the WT (bWT). In-frame deletions were identified by PCR and confirmed by DNA sequencing of the chromosomal DNA flanking the deletion.

Gallocin A production assays

32 Briefly, one colony of the indicator strain, here *Streptococcus gallolyticus subps.*
33 *macedonicus (SGM)*, was resuspended in 2 mL THY, grown until exponential phase, poured
34 on a THY agar plate, the excess liquid was removed and left to dry under the hood for about
35 20 min. Using sterile tips, 5-mm-diameter wells were dug into the agar. Each well was then
36 filled with 80 µL of filtered supernatant from 5 h cultures (stationary phase) of *SGG* UCN34
37 WT or otherwise isogenic mutant strains and supplemented with Tween 20 at 0.1% final
38 concentration. Inhibition rings around the wells were observed the following morning after
39 overnight incubation at 37°C.
40
41 **Competition experiments**
42 *SGG* strains were inoculated from fresh agar plate at initial DO_{600} of 0.1 together with *E.*
43 *faecalis* OG1RF in THY medium and incubated for 4 h at 37°C in micro aerobiosis. After 4 h of
44 co-culture, the mixed cultures were serially diluted and plated on Enterococcus agar-
45 selective plates (BD Difco). On these plates, *SGG* exhibits a pale pink color while *E. faecalis*
46 exhibits a strong purple color. CFU were counted the next morning to determine the final
47 concentration in CFU/mL in each test sample.
48
49 **Analysis of gallocin A peptides by LC-MS**
50 *Sgg* UCN34 was grown in 500 mL of sterile THY supplemented with 5 nM synthetic GSP at
51 37 °C with 5% CO_2 for 12-16 h. The cultures were centrifuged at 4,000 x g for 20 min and the
52 supernatant was filtered through a sterile 0.22 µm polyethersulfone (PES) filter. Ammonium
53 sulfate was added to the filtered supernatants to give a 20% (wt/vol) concentration and
54 mixed by inversion until all ammonium sulfate salts went into solution. The solution was
55 stored at 4 °C for 1 h, followed by centrifugation at 4,000 × g for 20 min. The supernatants
56 were discarded, and the remaining pellet was dissolved in 100 mL DI water and placed in a 3
57 kDa MWCO dialysis tube. The dialysis tube was placed in a 500 mL graduated cylinder
58 containing distilled water and a stir bar. Dialysis was performed for 4 h with changing of DI
59 water every hour. The material in the dialysis tube was then lyophilized. A 5 mg/mL solution
60 of the lyophilized material was prepared in 75:25 (H_2O:ACN) and 50 µL were injected into an
61 Agilent Technologies 6230 time of flight mass spectrometer (an HRMS system) with the
62 following settings for positive electrospray ionization (ESI+) mode: capillary voltage = 3,500
63 V; fragmentor voltage = 175 V; skimmer voltage = 65 V; Oct 1 RF Vpp = 750 V; gas

64 temperature = 325 °C; drying gas flow rate = 0.7 L/min; nebulizer; 25 lb/in2; acquisition time
65 = 17.5 min. An XBridge C18 column (5 µm, 4.6 x 150 mm) was used for the LC-MS analysis.
66
67 **Membrane permeabilization assays**
68 These assays were performed as described previously (28). Briefly, ANTS (fluorophore
69 probe) and DPX (quencher) were encapsulated into large unilamellar vesicles (LUVs) to
70 monitor membrane permeabilization induced by peptides. The LUVs were prepared at a
71 concentration of 10 mM lipid at a POPC:POPG molar ratio of 8:2 containing 20 mM ANTS
72 and 60 mM DPX. The multilamellar vesicle suspension was extruded through 0.4- and 0.2-
73 µm polycarbonate filters to produce LUVs of 200 ± 30 nm in diameter, as measured by DLS.
74 The unencapsulated ANTS and DPX were removed by gel filtration through a Sephadex G-25
75 column 5 mL (Cytiva, USA). For permeabilization assays, LUVs were incubated in buffer at
76 0.45 mM lipids at 25 ◦C in a 101-QS cuvette (Hellma, France) and under constant stirring.
77 The excitation wavelength was set to 390 nm and the emission of ANTS was continuously
78 measured at 515 nm. The maximum intensity of permeabilization, corresponding to the
79 maximum recovery of ANTS fluorescence was measured after addition of 0.12% (2 mM) of
80 Triton X100.
81
82 **Generation of gallocin resistant mutants**
83 In order to generate gallocin resistant mutants, we concentrated *SGG* supernatant 200
84 times by precipitation with 20% of ammonium sulfate. By serial 2-fold dilutions, we showed
85 that this supernatant was approximatively 64 times more concentrated than the original
86 supernatant (Fig. S5A). Fourteen resistant mutants (named RSM1 to 14) of *S. gallolyticus*
87 *subsp. macedonicus* parental strain CIP105683T, the species showing the highest sensitivity
88 to gallocin A, were selected on THY agar plates containing 10% of this concentrated
89 supernatant. Twelve of them were confirmed to be gallocin resistant by growth in THY
90 supplemented with the supernatant of *SGG* WT, containing gallocin, and 0.01% of Tween20,
91 which is necessary for gallocin A activity (Fig. S4B and C). As an important control, the same
92 experiment was performed after precipitation of the Δ*blp* supernatant that does not
93 produce gallocin A. *SGM* WT was re-isolated on this plate and a single colony was stocked
94 and sequenced with the RSM mutants as described below.
95

96 **Sequencing and SNP localization**

97 Whole-genome sequencing of the control *SGM* WT, re-isolated from *Δblp* plate as described
98 in the section above, and of RSM mutants was performed using Illumina technology and
99 compared with the genome of the parental strain *SGM* CIP105683T that was *de novo*
100 assembled using PacBio sequencing. The assembly was performed with Canu 1.6. (29)
101 leading to a main chromosome of 2,210,410bp and a plasmid of 12729bp (HE613570.1). The
102 annotation was subsequently made with Prokka (30) before a variant calling was performed
103 using the Sequana (31) variant calling pipeline. Of note, variants were called with a
104 minimum frequency of 10% and a minimum strand balance of 0.2. Many mutations,
105 probably due to the different method used for the sequencing of the reference sequence,
106 were present in the control *SGM* WT strain used as control and the RSM mutants.
107 Therefore, only RSM specific mutations occurring at a frequency>0.5 as compared to control
108 SGM WT were taken into account for this analysis and are shown in Table 2.

ACKNOWLEDGEMENTS

We would like to thank particularly Tarek Msadek for careful and critical reading of the manuscript. This study has been funded by the Institut National contre le Cancer (INCA) PLBIO 16-025 attributed to S. Dramsi and from the French Government's Investissement d'Avenir program, Laboratoire d'Excellence "Integrative Biology of Emerging Infectious Diseases (grant n° ANR-10-LABX-62-IBEID). This study was also funded by the National Science Foundation (NSF, CHE-1808370, to Y.T).

REFERENCES

1. Aymeric L, Donnadieu F, Mulet C, du Merle L, Nigro G, Saffarian A, Bérard M, Poyart C, Robine S, Regnault B, Trieu-Cuot P, Sansonetti PJ, Dramsi S. 2018. Colorectal cancer specific conditions promote Streptococcus gallolyticus gut colonization. Proc Natl Acad Sci U S A 115:E283–E291.

2. Hill D, O'Connor PM, Altermann E, Day L, Hill C, Stanton C, Ross RP. 2020. Extensive bacteriocin gene shuffling in the Streptococcus bovis/Streptococcus equinus complex reveals gallocin D with activity against vancomycin resistant enterococci. Sci Rep 10:13431.

3. Alvarez-Sieiro P, Montalbán-López M, Mu D, Kuipers OP. 2016. Bacteriocins of lactic acid bacteria: extending the family. Appl Microbiol Biotechnol 100:2939–2951.

4. Proutière A, du Merle L, Périchon B, Varet H, Gominet M, Trieu-Cuot P, Dramsi S. 2021. Characterization of a Four-Component Regulatory System Controlling Bacteriocin Production in Streptococcus gallolyticus. mBio 12:e03187-20.

5. Harrington A, Proutière A, Mull RW, du Merle L, Dramsi S, Tal-Gan Y. 2021. Secretion, Maturation, and Activity of a Quorum Sensing Peptide (GSP) Inducing Bacteriocin Transcription in Streptococcus gallolyticus. mBio 12:e03189-20.

6. Oppegård C, Rogne P, Emanuelsen L, Kristiansen PE, Fimland G, Nissen-Meyer J. 2007. The Two-Peptide Class II Bacteriocins: Structure, Production, and Mode of Action. J Mol Microbiol Biotechnol 13:210–219.

7. Kjos M, Oppegård C, Diep DB, Nes IF, Veening J-W, Nissen-Meyer J, Kristensen T. 2014. Sensitivity to the two-peptide bacteriocin lactococcin G is dependent on UppP, an enzyme involved in cell-wall synthesis. Mol Microbiol 92:1177–1187.

8. Landeta C, Boyd D, Beckwith J. 2018. Disulfide bond formation in prokaryotes. Nat Microbiol 3:270–280.

9. Meehan BM, Landeta C, Boyd D, Beckwith J. 2017. The Disulfide Bond Formation Pathway Is Essential for Anaerobic Growth of Escherichia coli. J Bacteriol 199:e00120-17.

10. Mirdita M, Schütze K, Moriwaki Y, Heo L, Ovchinnikov S, Steinegger M. 2022. ColabFold: making protein folding accessible to all. Nat Methods 19:679–682.

11. Kommineni S, Bretl DJ, Lam V, Chakraborty R, Hayward M, Simpson P, Cao Y, Bousounis P, Kristich CJ, Salzman NH. 2015. Bacteriocin production augments niche competition by enterococci in the mammalian gastrointestinal tract. Nature 526:719–722.

12. Heilbronner S, Krismer B, Brötz-Oesterhelt H, Peschel A. 2021. The microbiome-shaping roles of bacteriocins. Nat Rev Microbiol 19:726–739.

13. Rogne P, Fimland G, Nissen-Meyer J, Kristiansen PE. 2008. Three-dimensional structure of the two peptides that constitute the two-peptide bacteriocin lactococcin G. Biochim Biophys Acta 1784:543–554.

14. Rogne P, Haugen C, Fimland G, Nissen-Meyer J, Kristiansen PE. 2009. Three-dimensional structure of the two-peptide bacteriocin plantaricin JK. Peptides 30:1613–1621.

15. Fimland N, Rogne P, Fimland G, Nissen-Meyer J, Kristiansen PE. 2008. Three-dimensional structure of the two peptides that constitute the two-peptide bacteriocin plantaricin EF. Biochim Biophys Acta 1784:1711–1719.

16. Acedo JZ, Towle KM, Lohans CT, Miskolzie M, McKay RT, Doerksen TA, Vederas JC, Martin-Visscher LA. 2017. Identification and three-dimensional structure of carnobacteriocin XY, a class IIb bacteriocin produced by Carnobacteria. FEBS Lett 591:1349–1359.

17. Nissen-Meyer J, Oppegård C, Rogne P, Haugen HS, Kristiansen PE. 2010. Structure and Mode-of-Action of the Two-Peptide (Class-IIb) Bacteriocins. Probiotics Antimicrob Proteins 2:52–60.

18. Marciset O, Jeronimus-Stratingh MC, Mollet B, Poolman B. 1997. Thermophilin 13, a Nontypical Antilisterial Poration Complex Bacteriocin, That Functions without a Receptor*. J Biol Chem 272:14277–14284.

19. Flynn S, van Sinderen D, Thornton GM, Holo H, Nes IF, Collins JK. 2002. Characterization of the genetic locus responsible for the production of ABP-118, a novel bacteriocin produced by the probiotic bacterium Lactobacillus salivarius subsp. salivarius UCC118. Microbiol Read Engl 148:973–984.

20. Garneau S, Ference CA, van Belkum MJ, Stiles ME, Vederas JC. 2003. Purification and characterization of brochocin A and brochocin B(10-43), a functional fragment generated by heterologous expression in Carnobacterium piscicola. Appl Environ Microbiol 69:1352–1358.

21. Siragusa GR, Cutter CN. 1993. Brochocin-C, a new bacteriocin produced by Brochothrix campestris. Appl Environ Microbiol 59:2326–2328.

22. Dubrac S, Boneca IG, Poupel O, Msadek T. 2007. New Insights into the WalK/WalR (YycG/YycF) Essential Signal Transduction Pathway Reveal a Major Role in Controlling Cell Wall Metabolism and Biofilm Formation in Staphylococcus aureus. J Bacteriol 189:8257–8269.

23. Dubrac S, Bisicchia P, Devine KM, Msadek T. 2008. A matter of life and death: cell wall homeostasis and the WalKR (YycGF) essential signal transduction pathway. Mol Microbiol 70:1307–1322.

24. Hu J, Zhang X, Liu X, Chen C, Sun B. 2015. Mechanism of reduced vancomycin susceptibility conferred by walK mutation in community-acquired methicillin-resistant Staphylococcus aureus strain MW2. Antimicrob Agents Chemother 59:1352–1355.

25. Peng H, Hu Q, Shang W, Yuan J, Zhang X, Liu H, Zheng Y, Hu Z, Yang Y, Tan L, Li S, Hu X, Li M, Rao X. 2017. WalK(S221P), a naturally occurring mutation, confers vancomycin resistance in VISA strain XN108. J Antimicrob Chemother 72:1006–1013.

26. Yin Y, Chen H, Li S, Gao H, Sun S, Li H, Wang R, Jin L, Liu Y, Wang H. 2019. Daptomycin resistance in methicillin-resistant Staphylococcus aureus is conferred by IS256 insertion in the promoter of mprF along with mutations in mprF and walK. Int J Antimicrob Agents 54:673–680.

27. Danne C, Guérillot R, Glaser P, Trieu-Cuot P, Dramsi S. 2013. Construction of isogenic mutants in Streptococcus gallolyticus based on the development of new mobilizable vectors. Res Microbiol 164:973–978.

28. Voegele A, Sadi M, O'Brien DP, Gehan P, Raoux-Barbot D, Davi M, Hoos S, Brûlé S, Raynal B, Weber P, Mechaly A, Haouz A, Rodriguez N, Vachette P, Durand D, Brier S, Ladant D, Chenal A. 2021. A High-Affinity Calmodulin-Binding Site in the CyaA Toxin Translocation Domain is Essential for Invasion of Eukaryotic Cells. Adv Sci Weinh Baden-Wurtt Ger 8:2003630.

29. Koren S, Walenz BP, Berlin K, Miller JR, Bergman NH, Phillippy AM. 2017. Canu: scalable and accurate long-read assembly via adaptive k-mer weighting and repeat separation. Genome Res 27:722–736.

30. Seemann T. 2014. Prokka: rapid prokaryotic genome annotation. Bioinforma Oxf Engl 30:2068–2069.

31. Cokelaer T, Desvillechabrol D, Legendre R, Cardon M. 2017. "Sequana": a Set of Snakemake NGS pipelines. J Open Source Softw 2:352.

FIGURE LEGENDS

Fig. 1. Gallocin A is a two-peptide bacteriocin.

A) The core operon encoding gallocin A peptides and the immunity protein in *SGG* strain UCN34. Gallocin genes are indicated in red and renamed *gllA1* and *gllA2* according to (2). **B)** Agar diffusion assay to test gallocin activity from supernatants of UCN34 WT, Δ*gllA1*, Δ*gllA2* et Δ*blp* against gallocin-sensitive *S. gallolyticus subsp. macedonicus (SGM)* strain. **C)** and **D)** Growth curves of *SGG* Δ*blp, S. agalactiae* A909 and *L. lactis* NZ9000 containing an empty plasmid (p) or a plasmid expressing *gip* (p-*gip*) in THY supplemented with supernatant of Δ*blpS* (a strain overproducing gallocin, "+gallocin") or Δ*blp* (gallocin deletion mutant, "-gallocin") and 0.01% of tween 20.

Fig. 2. Gallocin A is active against most streptococci, lactococci and enterococci.

Phylogenetic tree based on the 16S RNA sequence (from the Silva online database) of different bacterial species that are resistant (in red) or sensitive (in green) to gallocin, as determined by agar diffusion assay (Fig. S2).

Fig. 3. Gallocin A can permeabilize bacterial membranes and lipid vesicles.

Fluorescence of the voltage-sensitive DiBac4(3) (**A**) or the membrane impermeant propidium iodide PI (**B**) after resuspension of *Enterococcus faecalis* OG1RF in supernatant of UCN34 WT, Δ*blp* (-gallocin) and Δ*blpS* (overexpressing gallocin). **C-D)** Measure of the fluorescence corresponding to the release of ANTS (ex: 390nm, em: 515nm) encapsulated in large unilamellar vesicles after addition of *SGG* supernatant or Triton X-100 (positive control). **C**: At 60 s, Triton or the supernatant of *SGG* UCN34 WT, or Δ*blp*, or WT 30X (concentrated 30 times) or Δ*blp* 30X, were added to the liposomes. **D**: At 60 s (SN1), the supernatant of Δ*gllA1* or Δ*gllA2* was added to the lipid vesicle suspension. At 200 s (SN2), the supernatant of the other strain is added. AU: Arbitrary Unit.

Fig. 4. Gallocin A peptides possess a disulfide bridge important for structure and activity.

A) Agar diffusion assay to test gallocin activity from supernatants of *SGG* WT or Δ*blpS* supplemented or not with 50mM of DTT **B)** Schematic representation of the gallocin

genomic locus and pBLAST domain identification in BlpT protein. **C)** Recovered *E. faecalis* after co-culture at 1:1 ratio for 4 h with *SGG* WT, Δ*blp,* Δ*blpT* and WT revertant from *blpT* deletion.

Fig. 5. **Structural models of GllA1 and GllA2 predicted using ColabFold.** Pro- and mature forms of GllA1 (A) and GllA2 (B) using ColabFold and visualization was obtained with PyMOL (version 2.5.2 The PyMOL Molecular Graphics System, Version 2.0 Schrödinger, LLC). All representations are colored with predicted lDDT from a score of 30% (red) to 100% (blue). For the pro-GllA1 and pro-GllA2, glycine doublet is colored in green. The disulfide bridges are represented in stick.

Fig. 6. Structural models of GIP and its interactions with GllA1, GllA2. A) ColabFold modelling of GIP and visualization with PyMOL. **B, C, D)** ColabFold modelling of the interaction between GllA1/GllA2 (**B**), GIP/GllA1 (**C**), GIP/GllA2 (**D**), and GllA1/GIP/GllA2 (**E**) interaction models aligned on the Cα of each GIP.

Fig. 7. Gallocin A-resistant mutants (RSM) forms aggregates and exhibit morphological defects as compared to the parental gallocin A-sensitive strain *SGM*.
Epifluorescence microscopy images of *SGM* WT and RSM 1 to 12 labelled with the Wheat Germ Agglutinin-488, a fluorescent peptidoglycan dye.

SUPPLEMENTARY FIGURE LEGENDS

Fig. S1. Gallocin A is active in a broad range of pH and heat-stable

A) Agar diffusion assay to test gallocin activity from supernatants of UCN34 WT and Δ*blp* at different pH against *SGM*, a gallocin A-sensitive bacterium. The initial supernatant from an overnight culture (left well) had a pH of 5.4. pH was then adjusted to 2-12 using HCl or NaOH. **B)** Supernatant was heated at 80°C for indicated times and tested as in (A).

Figure S2: Gallocin A spectrum of action

Agar diffusion assay using UCN34 WT and Δ*blp* supernatant against various bacterial species.

Fig. S3: LC-MS analysis of the two components comprising gallocin A indicating that both peptides contain a disulfide bridge.

Left Panel: Top – GllA2 structure, molecular formula and molecular weight (with disulfide bridge); Middle – Mass Spectrum showing the $MH_3^{+3}/3$ and $MH_4^{+4}/4$ masses observed for GllA2; Bottom – LC chromatogram showing the peak where GllA2 was detected. Right Panel: Top – GllA1 structure, molecular formula and molecular weight (with disulfide bridge); Middle – Mass Spectrum showing the $MH_2^{+2}/2$ and $MH_3^{+3}/3$ masses observed for GllA1; Bottom – LC chromatogram showing the peak where GllA1 was detected.

Fig. S4: Structural models of GllA1, GllA2 and GIP alone or in complex with each over. All representations are colored with predicted lDDT from a score of 30% (red) to 100% (blue). The disulfide bond is visible in stick representation for GllA1 and GllA2.

Fig. S5: Obtention of 12 spontaneous mutants (RSM) resistant to gallocin A as compared to the parental sensitive strain *SGM*.

A) Agar diffusion assay against *S. macedonicus* using serial two-fold dilutions of *Sgg* supernatant concentrated (SN 200X) or not (SN 1X) by ammonium sulfate precipitation. **B)** and **C)** Growth curves for the 12 gallocin A- resistant mutants in the presence or absence of gallocin A (THY medium supplemented with 30% of *SGG* WT/Δ*blp* supernatant)

Fig. S6: Amino acid changes in WalK, WalR or Aggregation Promoting Factor (APF) in RSM mutants as compared to the parental SGM (WT)

Comparison of the primary amino acid sequence of WalK (A), WalR (B), and the aggregation promoting factor (C) found in RSM mutants to their WT counterpart. Putative domains of these proteins, identified by BLAST, are shown in red (HATPase_C: smart00387 ; REC: cd17614 ; Helix-turn-helix: pfam00486 ; LysM: cd00118 and Lysozyme-like: cd13925). Putative residues important for the protein activity, identified by BLAST, are indicated by a dark arrowhead.

Fig. S7: Putative structure of two-component bacteriocins

Structural models of mature forms of the two peptides composing the two-component bacteriocins ABP118, Brochocin C and Thermophilin 13 using ColabFold. The amino acid sequence following the first glycine doublet (in bold) was considered as the mature form of the peptides. Uniprot accession numbers: ABP118: Q8KWI0; Q8KWH9. Brochocin C: O85756; O85757. Thermophilin 13: O54454; O54455. All representations are colored with predicted lDDT from a score of 30% (red) to 100% (blue). The disulfide bond is visible in stick representation for all the peptides except BrcB.

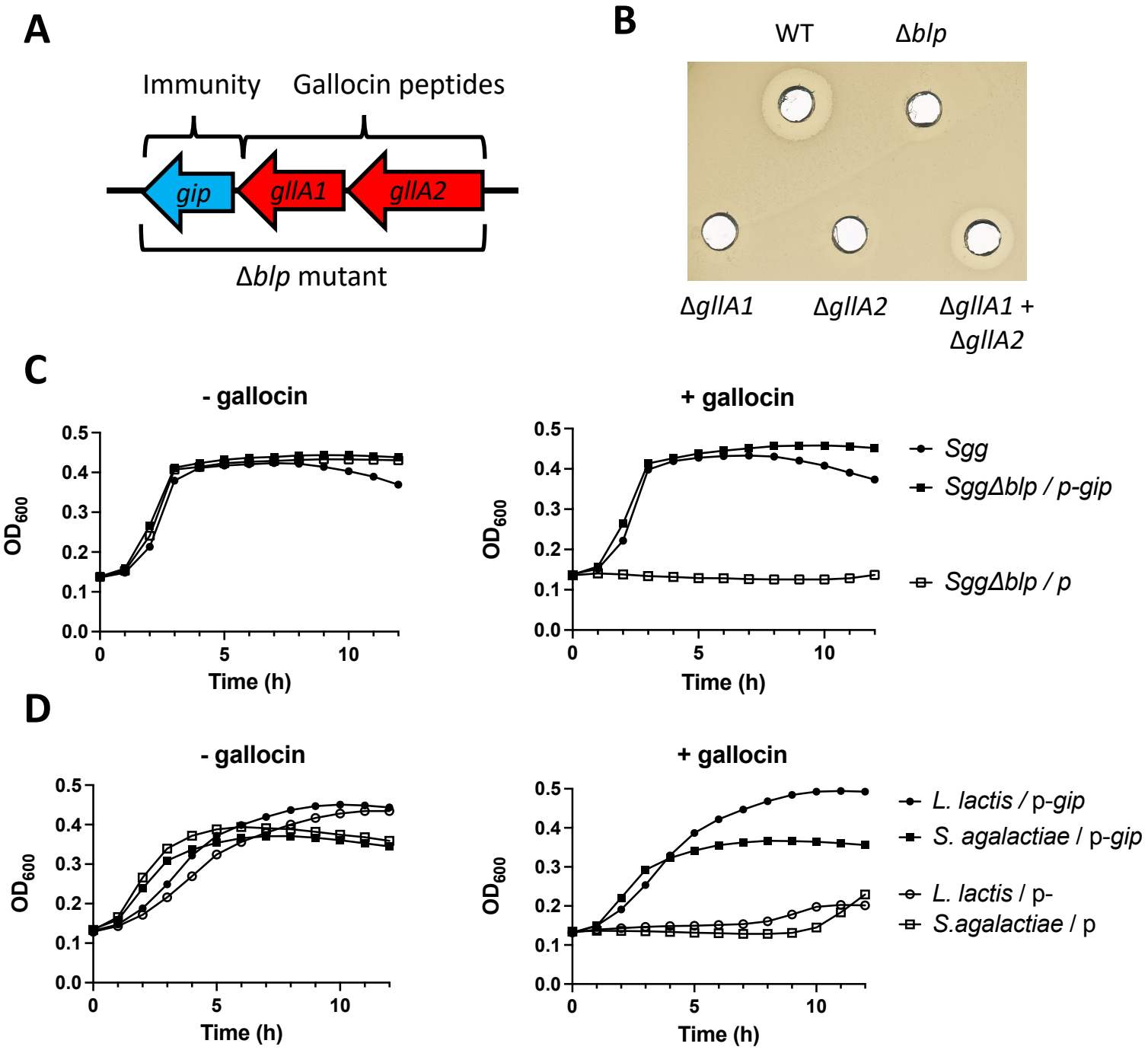

Figure 1 : Gallocin A is a two-peptide bacteriocin

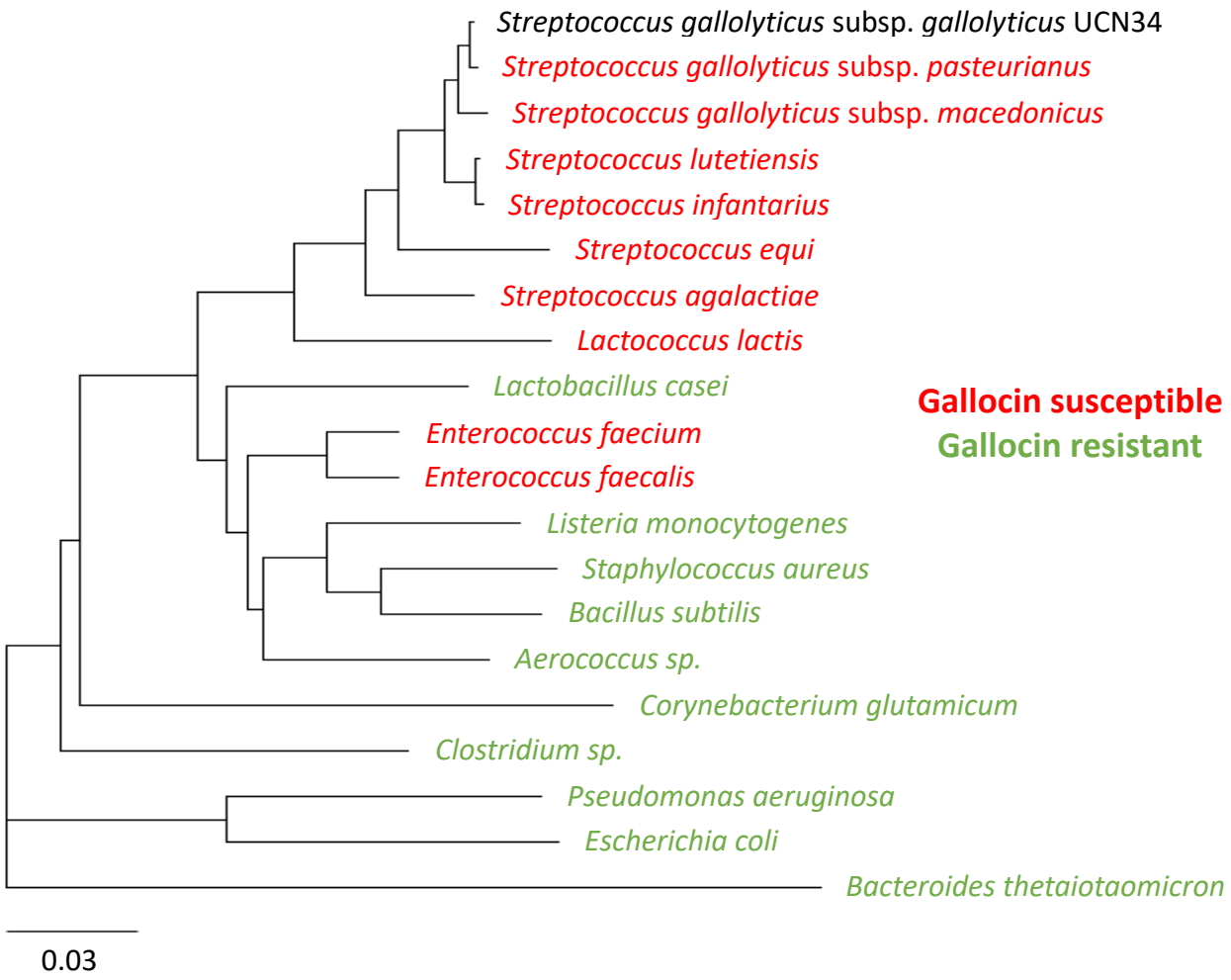

Figure 2 : Gallocin A is active against most streptococci, lactococci and enterococci.

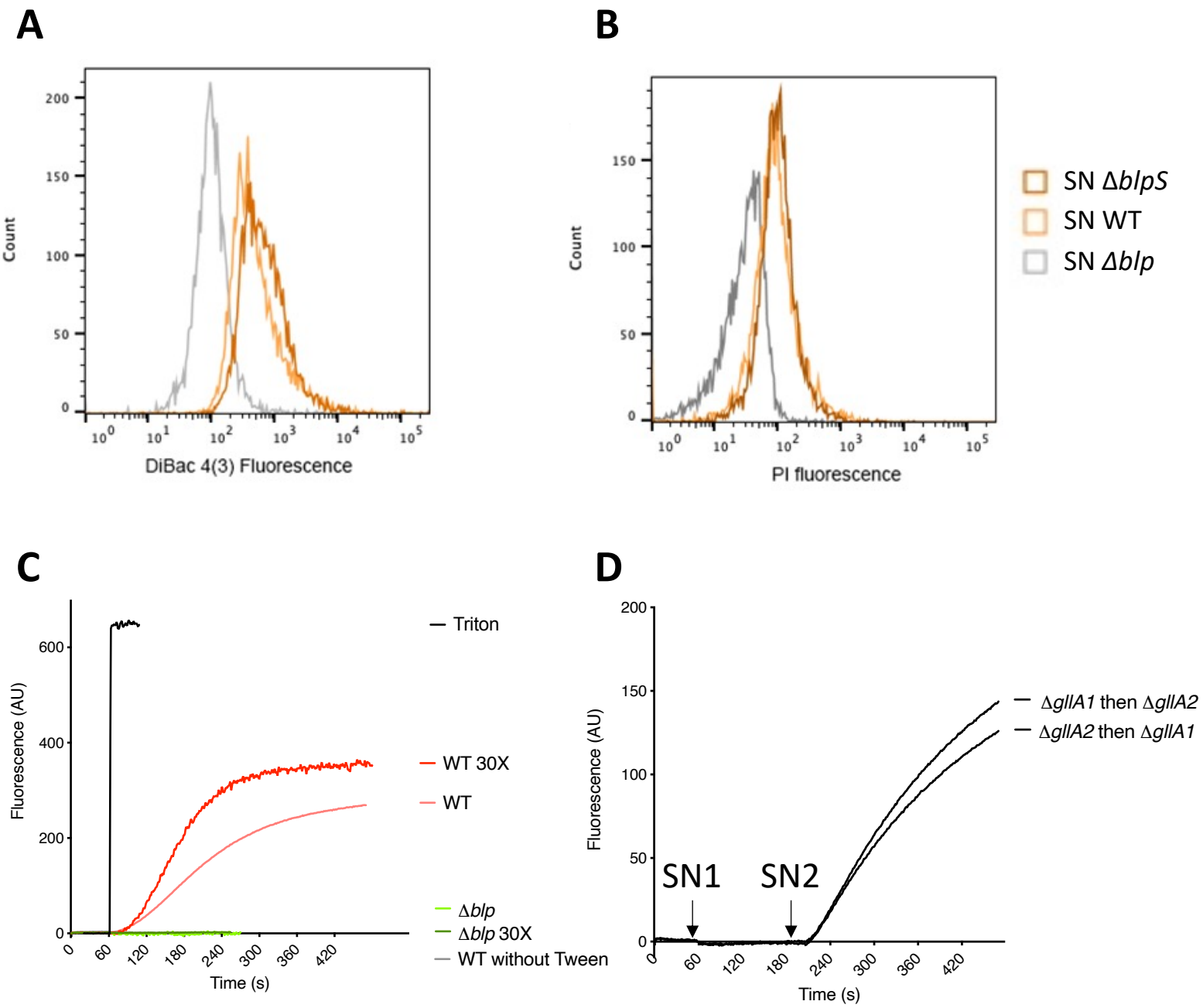

Figure 3: Gallocin A can permeabilize bacterial membranes and lipid vesicles.

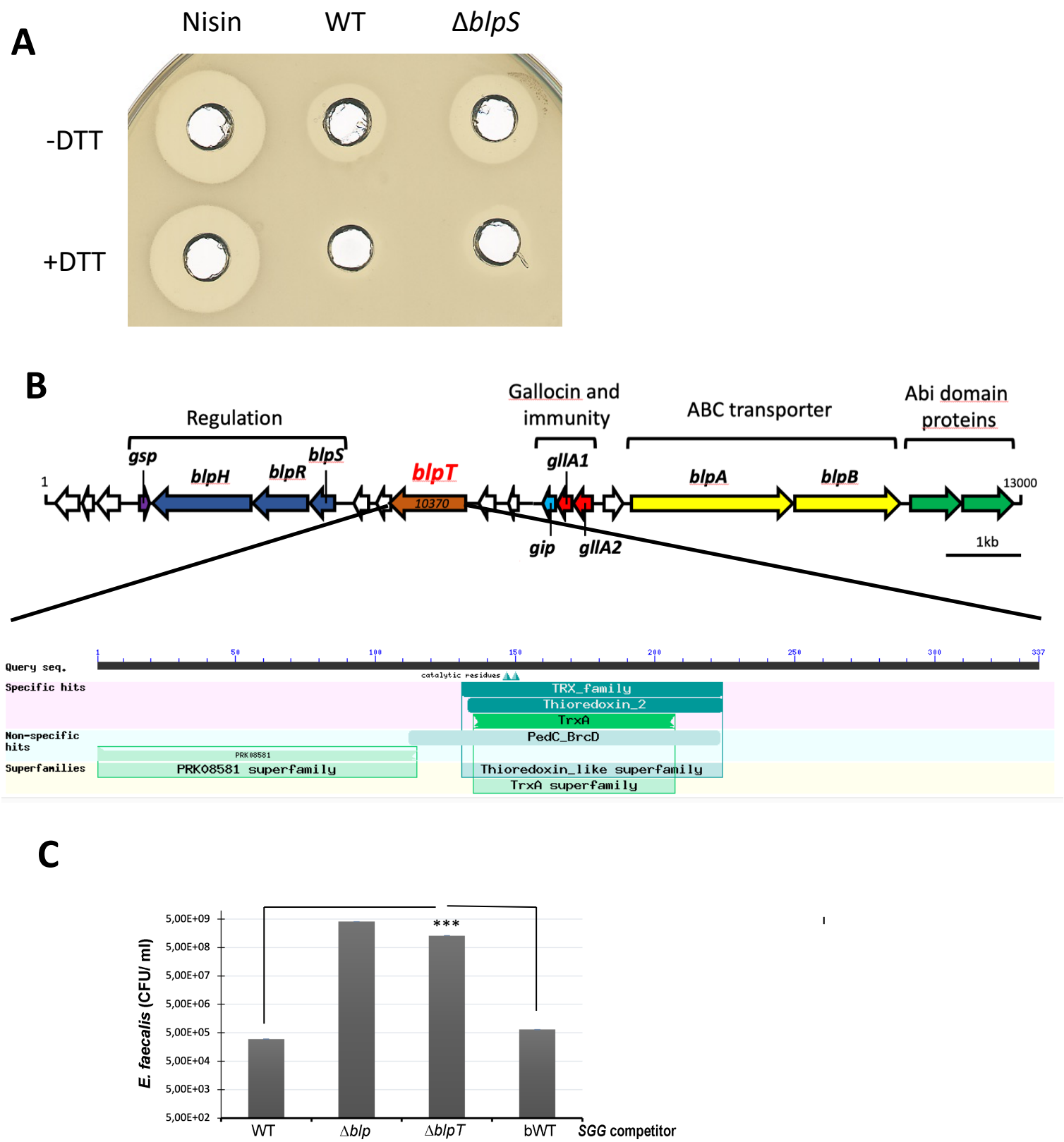

Figure 4: Gallocin A peptides possess a disulfide bond important for structure and activity.

A

Pro-GllA1

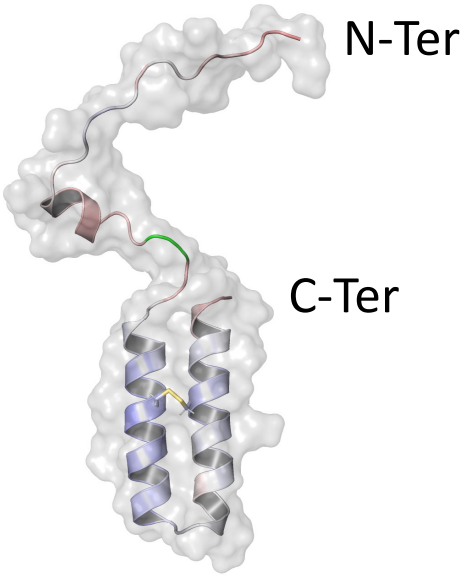

GllA1

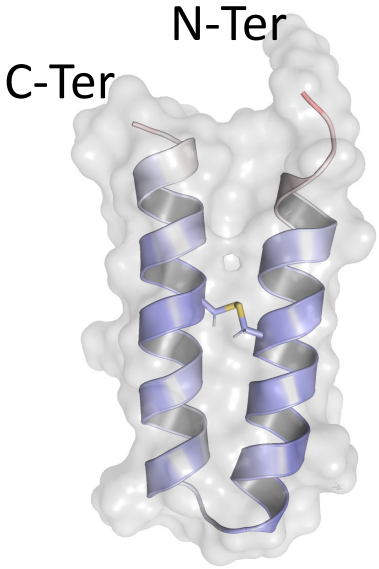

42 AA
MM 3.75 kDa

GllA1

MSLNKFTNFQELDKNHLQTISGG**KGNMGSAIGGCIGGVLLAAATGPITGGGA**
AMICVASGISAYL

B

Pro-GllA2

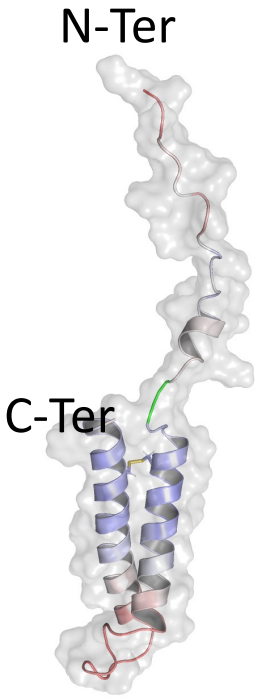

GllA2

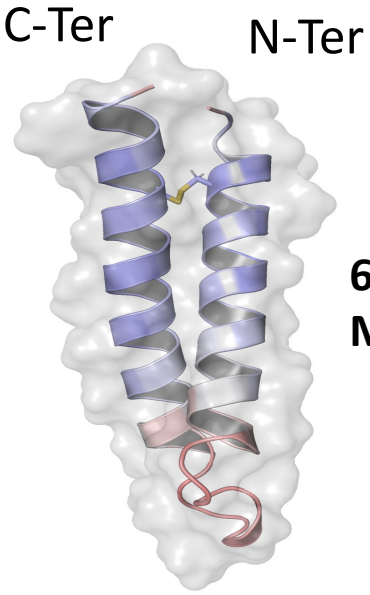

60 AA
MM 5.5 kDa

GllA2

MNTKTFEQFDVMTDEALSKVEGG**YSKTDCLNAMITGIAGGIVAGGTGAGLVT**
LGVAGLPGAFVGAHIGAIGGGATCVGGMLFN

Figure 5: Structural models of GllA1 and GllA2 predicted using Colabfold.

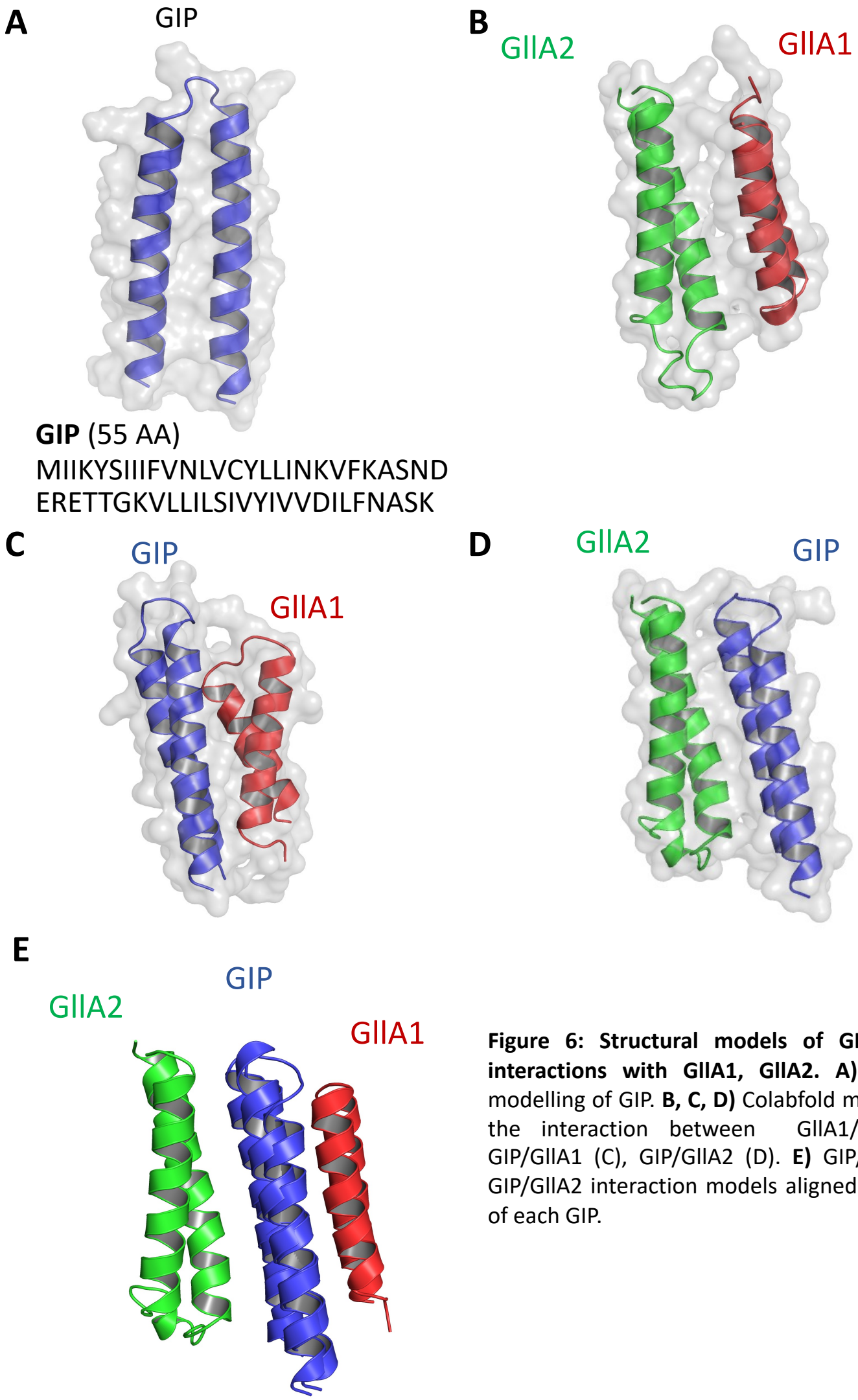

GIP (55 AA)
MIIKYSIIIFVNLVCYLLINKVFKASND
ERETTGKVLLILSIVYIVVDILFNASK

Figure 6: Structural models of GIP and its interactions with GIIA1, GIIA2. A) Colabfold modelling of GIP. **B, C, D)** Colabfold modelling of the interaction between GIIA1/GIIA2 (B), GIP/GIIA1 (C), GIP/GIIA2 (D). **E)** GIP/GIIA2 and GIP/GIIA2 interaction models aligned on the Cα of each GIP.

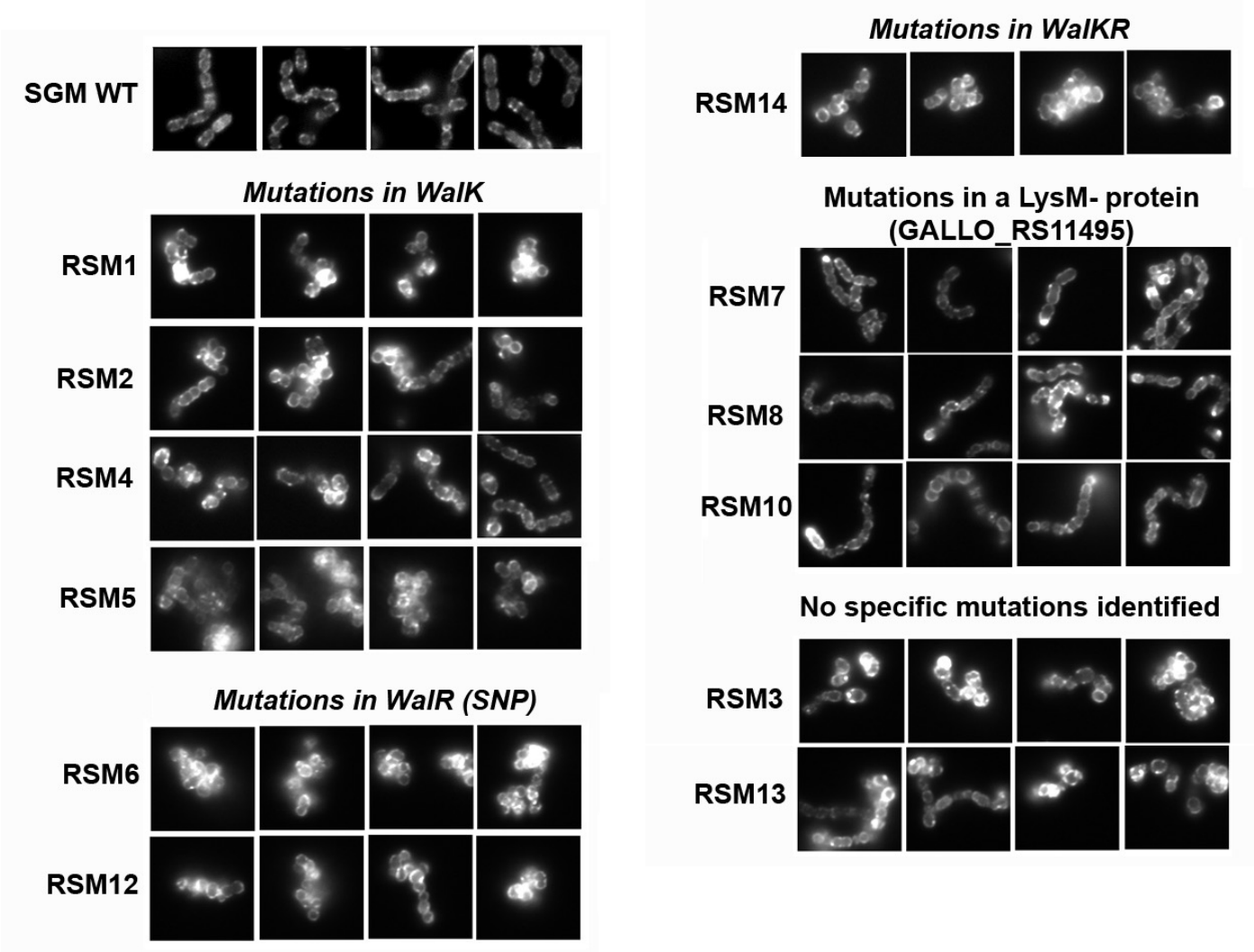

Figure 7: RSM mutants form aggregates as compared to the parental *SGM* WT. Epifluorescence microscopy images of *S. gallolyticus subsp. macedonicus (SGM)* WT and RSM 1 to 12 labelled with the Wheat Germ Agglutinin coupled to Alexa 488, a fluorescent lectin binding to the peptidoglycan.

Table 1: List of strains and primers

Number	Strains	Source
	***S. gallolyticus* strains**	
NEM 2431	*S. gallolyticus* subspecies *gallolyticus* UCN34	(Rusniok et al., 2010)
NEM 4838	UCN34 Δ*blp*	(Aymeric et al., 2018)
NEM 4694	UCN34 Δ*gllA1*	This work
NEM 4812	UCN34 Δ*gllA2*	This work
NEM 4988	UCN34 Δ*blpT* (*gallo_rs10370*)	This work
NEM 5097	UCN34 Δ*blpS*	(Proutiere *et al*., 2021)
NEM 1765	*S. gallolyticus* subspecies *macedonicus*	CIP 105683T
150507100801	*S. gallolyticus* subspecies *pasteurianus*	CNR collection (Cochin)
NEM 4801	UCN34 Δ*blp* pTCV P*tet-gip*	This work
NEM 4806	UCN34 Δ*blp* pTCV Ptet	This work
	Heterologous expression of immunity protein	
NEM 4828	*Lactococcus lactis* pTCV P*tet-gip*	This work
NEM 5667	Lactococcus lactis pTCV	This work
NEM4825	*Streptococcus agalactiae* A909 pTCV P*tet-gip*	This work
NEM3245	*Streptococcus agalactiae* A909 pTCV	This work
	Strains tested for gallocin sensitivity	
NEM 4825	*Streptococcus agalactiae* A909 pTCV Ptet-gip	Collection BBPG
NEM 1867	*Streptococcus infantarius*	CIP106105
NEM 640	*Streptococcus lutetiensis*	Collection BBPG
NEM 739	*Streptococcus equi*	Collection BBPG
NEM 2526	*S. agalactiae* A909	Collection BBPG
NEM 3525	*S. agalactiae* NEM316	Collection BBPG
NEM 2312	*S. agalactiae* BM110	Collection BBPG
NEM 409	*Enterococcus faecalis*	Collection BBPG
NEM 489	*Enterococcus faecium*	Collection BBPG
NEM 4906	*Lactococcus lactis*	Collection BBPG
NEM 4703	*Lactobacillus casei*	Collection BBPG
NEM 140	*Listeria monocytogenes* F6953	Collection BBPG
NEM 466	*Bacillus subtilis*	Collection BBPG
NEM 416	*Staphylococcus aureus* RN4220	Collection BBPG
NEM 453	*Escherichia coli*	Collection BBPG
NEM 761	*Aerococcus spp.*	Collection BBPG
NEM 486	*Pseudomonas aeruginosa*	Collection BBPG
NEM 602	*Corynebacterium glutamicum*	Collection BBPG
	Vancomycin resistant Enterrococcus	
CIP 103510	*E. faecium* (VanA)	Collection Institut Pasteur
CIP 111159	*E. faecalis* (VanB)	Collection Institut Pasteur
CIP 111253	*E. faecalis* (VanD)	Collection Institut Pasteur
CIP 111106	*E. faecalis* (VanE)	Collection Institut Pasteur
CIP 111107	*E. faecalis* (VanG)	Collection Institut Pasteur
	Competition expriment	
NEM 2829	*Enterococcus faecalis* OG1RF	Collection BBPG
	***Streptococcus gallolyticus* subspecies *macedonicus* mutants resistant to gallocin (RSM)**	
NEM 5627	RSM1	This work
NEM 5628	RSM2	This work
NEM 5629	RSM3	This work
NEM 5630	RSM4	This work
NEM 5631	RSM5	This work
NEM 5632	RSM6	This work
NEM 5633	RSM7	This work
NEM 5634	RSM8	This work
NEM 5636	RSM10	This work
NEM 5638	RSM12	This work
NEM 5639	RSM13	This work
NEM 5640	RSM14	This work

Primers	Sequence (5'-3')
	Deletions
gllA1	TTCT**GAATTC**GAAACTAGAACTATTGTGCC
	TTCTATAAGTATGCTGAAATACTCTCTCCTTATAAA
	TTTATAAGGAGAGAGTATTTCAGCATACTTATAGA
	TTCT**GGATCC**CAGGCAATATTATTGCCAT
gllA2	TTCT**GAATTC**TAATGCGGGAGTTTGCCT
	ACTCTCTCCTTATAAAATTATTGAATACCTCCCAATAA
	TTATTGGGAGGTATTCAATAATTTTATAAGGAGAGAGT
	TTCT**GGATCC**CAGGCAATATTATTGCCA
blpT (*gallo_RS10370*)	TTCT**GAATTC**AATCCCAGATAGACCGCC
	GCAACTGTTTTATCAATGGGCAGAGGAAAAGTAGCA
	TGCTACTTTTCCTCTGCCCATTGATAAAACAGTTGC
	TTCT**GGATCC**CGACAGACGGTATGTTAG
	Overexpression
gip	TTCT**GGATCC**ATTGGGAGGTATTCAAATGATTATAAAATATAG
	TTCT**CTGCAG**CAATAGTAATACATTAT

Table 2: Single nucleotide polymorphisms detected in RSM mutants as compared to the control *SGM* WT

Column1	level_0	chr	position	depth	reference	alternative	type	freebayes_score	strand_balance	fisher_pvalue	frequency	CDS_position	effect_type	codon_change	gene_name	mutation_type	prot_effect	prot_size	effect_impact	name
56	RSM-1_S3	assembly	1609857	141	GCCAGAT	GCCAGACCAGAT	INDEL	4416,47	0,471	1	0,98	961_962insTCTG	frameshift_variant	atc/aTCTGGtc	NPFEHBFA_01714		Leu323fs	450	HIGH	RSM-1_S3
57	RSM-1_S3	assembly	1967146	171	G	T	SNV	5614,57	0,402	0,405882353	0,99	17C>A	missense_variant	gCc/gAc	NPFEHBFA_02107	MISSENSE	Ala6Asp	123	MODERATE	RSM-1_S3
58	RSM-1_S3	assembly	1987074	309	TGT	TGGT	INDEL	5417,64	0,428	0,246009502	0,54	1987075_198707	intragenic_variant		NPFEHBFA_00018				MODIFIER	RSM-1_S3
79	RSM-2_S4	assembly	1609905	105	CGCTGATTGT	CGCTGATTGGCTGATTGT	INDEL	2980,49	0,447	0,4653761	0,90	910_911insCAAT	frameshift_variant	aca/aCAATCAGCca	NPFEHBFA_01714		Gly307fs	450	HIGH	RSM-2_S4
114	RSM-3_S5	assembly	1967146	191	G	T	SNV	6332,62	0,458	0,460732984	1,00	17C>A	missense_variant	gCc/gAc	NPFEHBFA_02107	MISSENSE	Ala6Asp	123	MODERATE	RSM-3_S5
8	RSM-4_S6	assembly	1609857	111	GCCAGATTGGTT	GCCAGATTGGTCCAGATTGGTT	INDEL	2566,58	0,488	0,36118636	0,74	956_957insACCA	frameshift_variant	aaa/aaACCAATCTGGa	NPFEHBFA_01714		Leu323fs	450	HIGH	RSM-4_S6
16	RSM-5_S7	assembly	1609830	150	G	A	SNV	4961,5	0,493	1	1,00	994C>T	stop_gained	Cag/Tag	NPFEHBFA_01714	NONSENSE	Gln332*	450	HIGH	RSM-5_S7
19	RSM-5_S7	assembly	2110152	194	C	T	SNV	6434,79	0,454	1	1,00	112G>A	missense_variant	Ggc/Agc	NPFEHBFA_02243	MISSENSE	Gly38Ser	139	MODERATE	RSM-5_S7
100	RSM-6_S8	assembly	1611243	145	G	A	SNV	4753,75	0,455	1	1,00	284C>T	missense_variant	gCa/gTa	NPFEHBFA_01715	MISSENSE	Ala95Val	236	MODERATE	RSM-6_S8
87	RSM-7_S9	assembly	59133	116	ATTTTTTGGTT	ATTTTTTTGGTT	INDEL	3769,47	0,47	1	0,99	112dupT	frameshift_variant	tgg/tTgg	NPFEHBFA_00076		Trp38fs	322	HIGH	RSM-7_S9
90	RSM-7_S9	assembly	1665912	103	C	T	SNV	3443,77	0,422	1	0,99	1665912C>T	intragenic_variant		NPFEHBFA_00018				MODIFIER	RSM-7_S9
91	RSM-7_S9	assembly	2167995	122	G	A	SNV	3983,79	0,475	1	1,00	403C>T	stop_gained	Caa/Taa	NPFEHBFA_02313	NONSENSE	Gln135*	197	HIGH	RSM-7_S9
138	RSM-8_S10	assembly	1028320	114	G	A	SNV	3821,48	0,421	1	1,00	107C>T	missense_variant	cCa/cTa	NPFEHBFA_01139	MISSENSE	Pro36Leu	87	MODERATE	RSM-8_S10
139	RSM-8_S10	assembly	2167972	163	G	T	SNV	5539,98	0,469	1	0,99	426C>A	stop_gained	taC/taA	NPFEHBFA_02313	NONSENSE	Tyr142*	197	HIGH	RSM-8_S10
68	RSM-9_S11	assembly	970200	81	G	A	SNV	1543,39	0,438	0,012693076	0,59	970200G>A	intragenic_variant		NPFEHBFA_00018				MODIFIER	RSM-9_S11
72	RSM-9_S11	assembly	1608485	93	C	T	SNV	3076,42	0,467	1	0,99	1608485C>T	intragenic_variant		NPFEHBFA_00018				MODIFIER	RSM-9_S11
128	RSM-10_S12	assembly	890476	125	A	G	SNV	4177,47	0,464	1	1,00	829A>G	missense_variant	Act/Gct	NPFEHBFA_00992	MISSENSE	Thr277Ala	366	MODERATE	RSM-10_S12
129	RSM-10_S12	assembly	1111112	98	GAAAAAATTG	GAAAAATTG	INDEL	3313,57	0,449	1	1,00	1111118delA	intragenic_variant		NPFEHBFA_00018				MODIFIER	RSM-10_S12
131	RSM-10_S12	assembly	2167989	131	C	T	SNV	4416,49	0,489	1	1,00	409G>A	missense_variant	Gaa/Aaa	NPFEHBFA_02313	MISSENSE	Glu137Lys	197	MODERATE	RSM-10_S12
107	RSM-11_S13	assembly	987794	132	ACCGA	ACGA	INDEL	4361,88	0,473	1	0,99	438delC	frameshift_variant	acc/	NPFEHBFA_01100		Glu147fs	520	HIGH	RSM-11_S13
119	RSM-12_S14	assembly	121316	138	T	G	SNV	4694,83	0,486	1	1,00	955T>G	stop_lost+splice_region_variant	Taa/Gaa	NPFEHBFA_00166	MISSENSE	Ter319Gluext*	318	HIGH	RSM-12_S14
122	RSM-12_S14	assembly	1611178	130	G	A	SNV	4376,41	0,408	1	1,00	349C>T	missense_variant	Cgt/Tgt	NPFEHBFA_01715	MISSENSE	Arg117Cys	236	MODERATE	RSM-12_S14
35	RSM-13_S15	assembly	404530	153	A	G	SNV	4984,05	0,49	1	1,00	314T>C	missense_variant	gTa/gCa	NPFEHBFA_00464	MISSENSE	Val105Ala	193	MODERATE	RSM-13_S15
36	RSM-13_S15	assembly	518528	144	C	G	SNV	4789,74	0,486	1	1,00	193C>G	missense_variant	Ccg/Gcg	NPFEHBFA_00589	MISSENSE	Pro65Ala	292	MODERATE	RSM-13_S15
38	RSM-13_S15	assembly	1847713	158	T	A	SNV	3277,13	0,408	0,867232731	0,62	1847713T>A	intragenic_variant		NPFEHBFA_00018				MODIFIER	RSM-13_S15
2	RSM-14_S16	assembly	1609544	106	G	A	SNV	3551,39	0,491	1	1,00	1280C>T	missense_variant	tCg/tTg	NPFEHBFA_01714	MISSENSE	Ser427Leu	450	MODERATE	RSM-14_S16
3	RSM-14_S16	assembly	2113956	123	C	T	SNV	4184,54	0,488	1	1,00	26G>A	missense_variant	gGa/gAa	NPFEHBFA_02247	MISSENSE	Gly9Glu	419	MODERATE	RSM-14_S16